International Journal of Geography, Geology and Environment

P-ISSN: 2706-7483
E-ISSN: 2706-7491
IJGGE 2022; 4(1): 154-160
Received: 12-02-2022
Accepted: 17-04-2022

M Sean Chenoweth
Ph.D., Department of Chemistry and Geosciences, Jacksonville State University, Jacksonville, Alabama, US

Corresponding Author:
M Sean Chenoweth
Ph.D., Department of Chemistry and Geosciences, Jacksonville State University, Jacksonville, Alabama, US

Morphometric quantification of cockpit karst in a Jamaican bauxite mining concession

M Sean Chenoweth

DOI: https://doi.org/10.22271/27067483.2022.v4.i1b.104

Abstract
A digital surface model (DSM) is used to characterize the landscape and topical karst landforms within a bauxite mining lease in north central Jamaica. Five case study sites are selected for detailed geomorphic analysis and cartographic visualization using a GIS. In Jamaica, tropical cockpit karst landscapes are composed of several landforms: cockpits, glades, corridors, saddles, and talus slopes. Evidence for the existence and quantification of these landforms is provided in this paper. Study sites have a mean basin area of 96,514 m^2, an average highest elevation of 541 m, mean lowest point of 444 m, with an average enclosed depression depth of 97 m. Depth and slope values within the study sites are consistent with previously published literature for cockpit karst landscapes. The literature also supports the findings in this study which are steep and convex slopes surrounding cockpit floors.

Keywords: Karst, cockpit, bauxite mining, Jamaica, conservation, elevation model

Introduction
The spatial analysis of cockpit karst landforms using a digital surface model (DSM) within a bauxite mining lease is the focus of this investigation. Cockpits are a part of the landscape in this region and the Cockpit Country Protected Area (CCPA) directly adjacent to the west of the bauxite mining lease boundary. Special Mining Lease 173 (SML-173) is a bauxite mining concession located within the Rio Bueno sub-Watershed Management Unit of north central Jamaica (Figure 1). SML-173 encompasses an area nearly 94 km^2 (9,400 hectares), covered in thick bauxitic soils in the glades and cockpits, and is underlain by the white limestone group (Miller, 2003) [1].

Sawkins (1869) [2] describes Cockpit land as a rough uncultivated track of country covered by fragmentary limestone, with pointed hills on narrow ridges, with deep precipitous hollows like inverted cones, or deep narrow troughs on which the forest trees thrive to the greatest perfection. Sawkins (1869, p.220) [2] explains the windward Cockpits occupying a section of Trelawny parish lying between the Alps and the parish line with St. Ann.

Aub (1969) [3] derives his depiction of the landscape from the exploration of 160 karst depressions. Cockpits are funnel or bowl-shaped basins varying from 30 m to 150 m in depth and up to several hundred meters in diameter. Surrounding slopes consist of solid limestone, are steep and convex, and often covered by boulders. Cockpit floors are areas with lower slope angles and are usually covered by soil or limestone debris while solid limestone floors are rare.

Cockpits have no integrated regional surface pattern, each is a closed depression, the bounding slopes are irregular in form, loose masses of rock of a variety of sizes are present, and the mean slope angle is about 30° (Smith *et al*. 1972) [4]. Tropical cockpit karst topography contains many closed depressions surrounded by conical hills, having steep sides and convex slopes, and star-shaped depressions having a conical or slightly concave floor (Monroe, 1972) [5].

Cockpits are large, enclosed depressions surrounded by residual carbonate hills (Chenoweth, 2003) [6], with steep to vertical sides (Versey, 1972) [7], and a slope range from 30° to 40° (Sweeting, 1958) [8], but some are bare and cliff-like exceeding 70° (Lyew-Ayee *et al*. 2006) [9].

Other landforms associated with tropical cockpit karst landscape include corridors which are low, narrow passes between two limestone hills connecting adjacent cockpits or glades while

saddles are minor topographic indentations between summits (Chenoweth, 2003) [6]. Saddle slopes are narrow, soil covered slopes often located below saddles, extending downslope to cockpit floors or glades with colluvium at their bases (Chenoweth, 2003) [6]. Talus slopes form from the accumulation of rubble eroded from cliff faces and bedrock disturbance by the windthrow of trees. Cliffs are rocky with extremely steep to vertical slopes and summits are the highest locations of hills. Ridge lines are the highest elevation contour between two drainage basins.

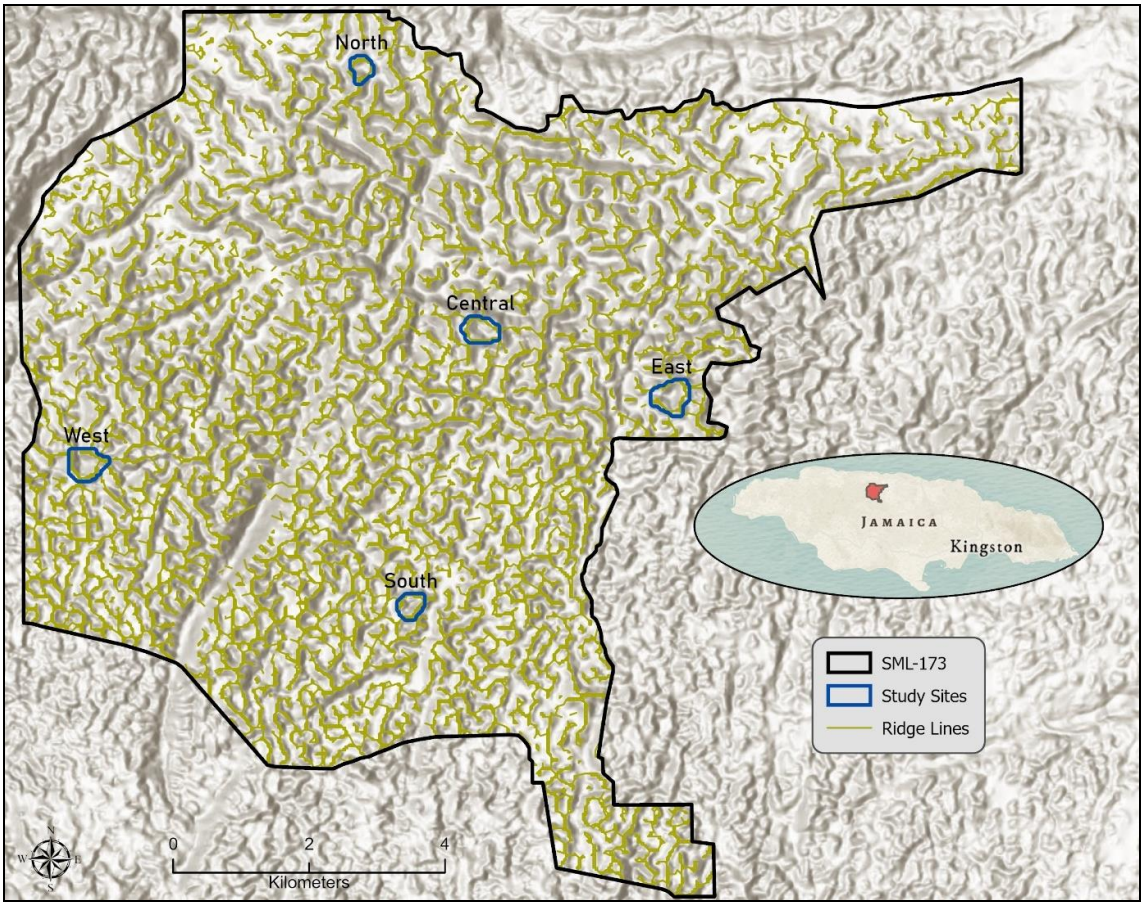

Fig 1: Location of the study area and sample sites in north central Jamaica, West Indies

Methods

ESRI ArcGIS Pro (version 2.8) professional desktop geographic information systems (GIS) software application is used to perform geoprocessing of spatially referenced datasets. The dataset is a digital surface model (DSM) with a horizontal spatial resolution of 30 meters (version 3.1, January 2021). This elevation grid was developed from the Panchromatic Remote-sensing Instrument for Stereo Mapping (PRISM), which is an optical sensor on board the Advanced Land Observing Satellite (ALOS-PRISM, 2022) [10]. The study area polygon (SML-173) was obtained from ArcGIS Online (ArcGIS Online, 2021) [11]. The Contour tool was used to create 5 m and 15 m contour intervals from the raster DSM. Landform profiles are created using the exploratory 3D Analysis Elevation Profile tool (Figure 4).

The Flow Direction tool creates a raster of flow direction layer from each cell to its downslope neighbors using the D8 method to its steepest downslope neighbor (ESRI Help). The Flow Accumulation tool calculates flow as the amassed weight of all cells flowing into each downslope cell in the output raster. The Raster Calculator is used to create a raster layer of zero flow accumulation for ridge lines. Raster ridges were converted vector polylines (Figure 1).

In conjunction with the flow direction raster the Basin tool was used on the DSM to delineate all drainage basins in SML-173. Individual study sites were selected and extracted from the basin layer and given generalized study site names for reference: North, East, Central, South, and West (Figure 1). A 45 m fixed distance buffer was used on the study sites layer to expand the smaller basin polygon to include local peaks of surrounding limestone hills. The Find Highest or Lowest Point tool was used with each buffered study site to expand and constrain the identification of these local elevation features.

Results

Elevation gradually increases from north to south across the study area with a mean of 449 m (asl) and a standard deviation of 100 m. Overall, topographic change inside SML-173 using the 30 m DSM ranges from 197 m to 690 m resulting in 493 m of relief. There are 1,158 independent drainage basins ranging in size from 907 m^2 to 868,080 m^2. Within the study area basins there are 512 sinks or topographically low spots.

The five sampled study areas (Figure 1) have an average basin area of 96,514 m^2, and a mean highest elevation of 541 m, mean lowest point of 444 m, with an average depth of 97 m (Table 1). Slopes associated with the five study areas are represented by a minimum mean of 2.26°, a maximum mean slope of 38.68°, an overall mean slope of 20.3°, and average slope standard deviation of 8.18° (Table 2).

Table 1: Study sites morphology and elevation summaries.

Site Name	Basin Perimeter (m)	Basin Area (m^2)	Highest Peak (m)	Lowest Point (m)	Depth (m)
North	1,144	47,168	354	267	87
East	1,807	134,249	609	520	89
Central	1,505	101,594	554	466	88
South	1,205	65,310	628	529	99
West	1,747	134,249	559	438	121
$\bar{x}$	1,482	96,514	541	444	97

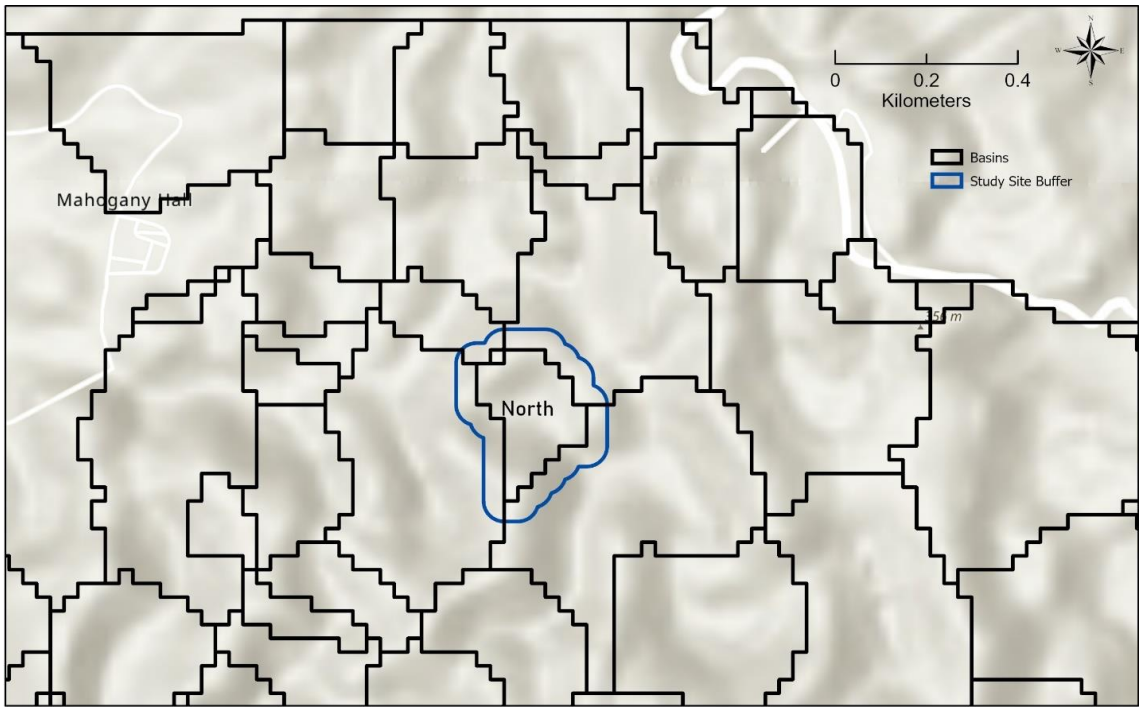

Fig 2: Illustrates the North study area with 45-meter buffered polygon and surrounding drainage basins. Arterial road is to the northeast (white line)

The North study area is slightly elongated north to south (Figure 2) and represents the smallest cockpit sample in this paper with a basin area of 47,168 m^2 (Table 1). The highest peak associated with this enclosed depression is located on the south end at 354 m while to lowest point is in the center at 267 m creating 87 m of relief. The minimum slope is 1.8°, the maximum slope is 34.5°, with a mean of 18.5° (Table 2).

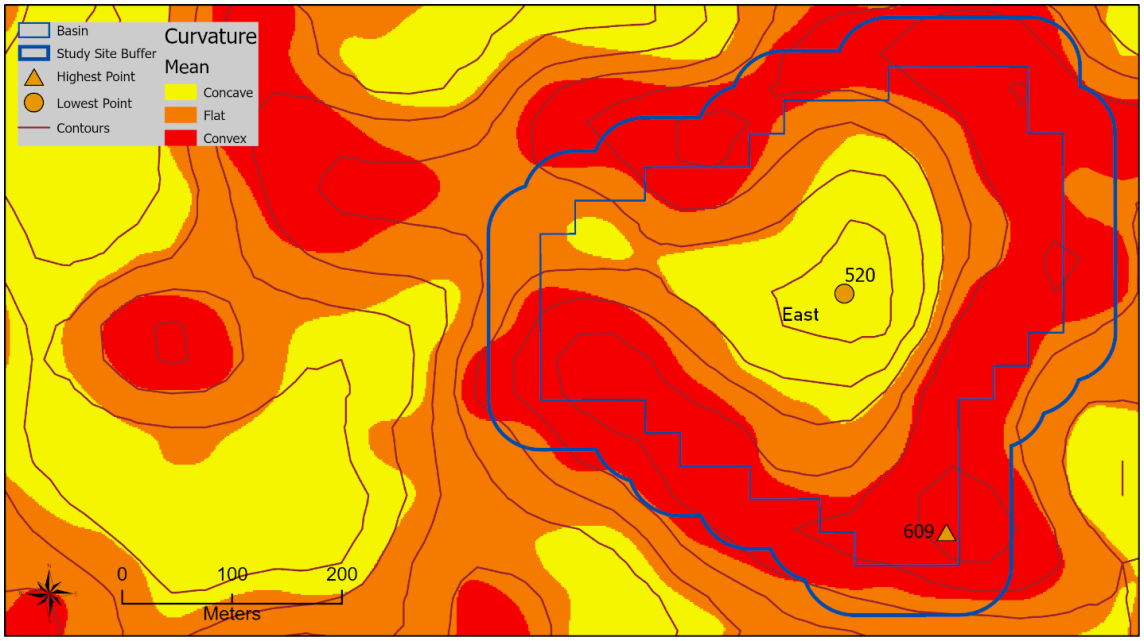

Fig 3: East study site curvature model with spot elevations in meters

The Eastern study site (Figure 3) is slightly larger than the western study site with an area of 134,249 m^2 (Table 1). The lowest point is 520 m, and the surrounding highest peak is 609 m yielding a maximum depth of 89 m for the Eastern basin study site. Slope values for the Eastern site range from a minimum value of 0.5° to 46.9° with an average of 19.5° (Table 2).

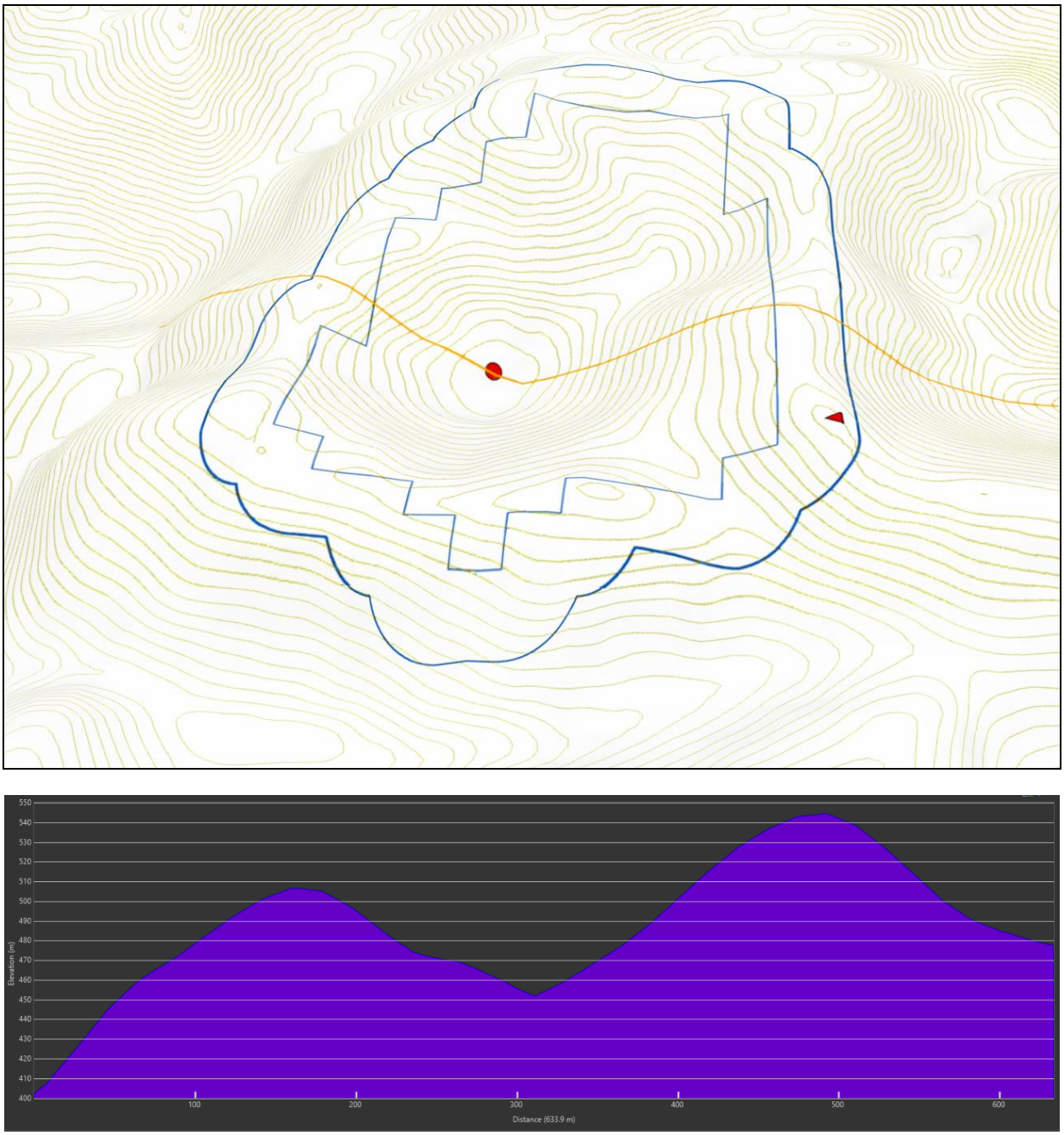

Fig 4: Central study site elevation profile (north to left). (Top) 3-D perspective of the cockpit with profile line (gold), study site buffer (outer polygon), basin (inner polygon), highest point (triangle), and lowest point (circle); scale varies in this perspective view. (Bottom) Elevation profile of gold line

The Central study site is illustrated by a 3D view of contours along with a profile of the depression and hills (Figure 4). The basin area is 101,594 m^2 and is closest to the average basin area (Table 1). The depth is 88 m calculated from the 554 m highest surrounding peak and 466 m low point. The average slope value for the Central study site is 18.2°, minimum of 4.8°, and maximum of 31.3° (Figure 2).

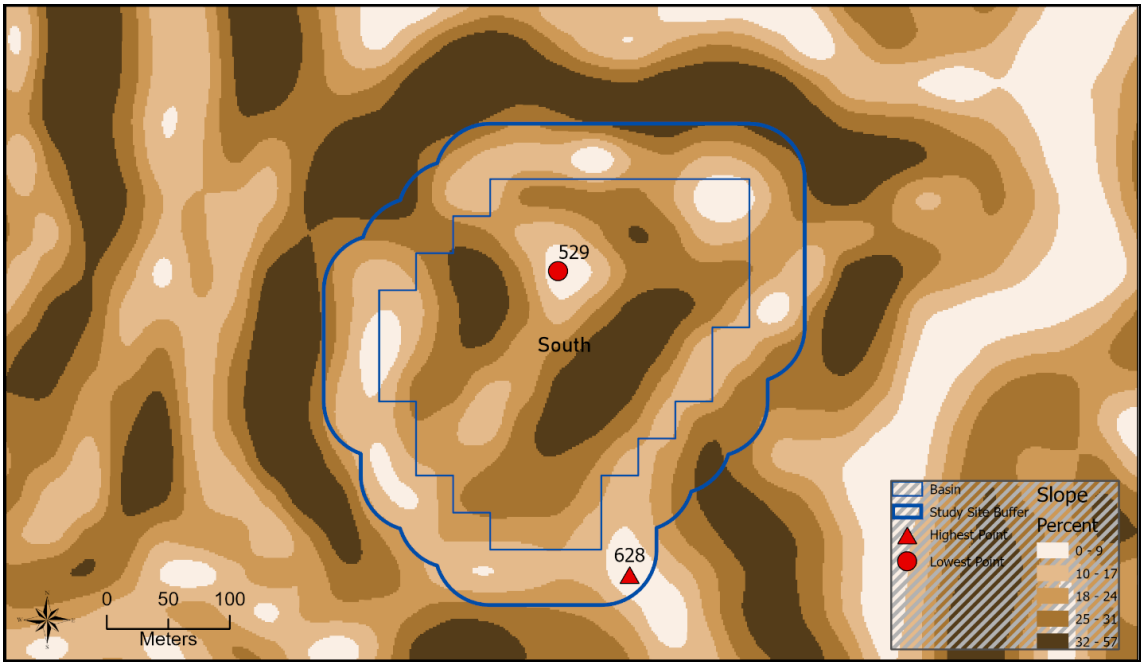

Fig 5: Slope model of the South study site within SML-173 with spot elevations in meters

The South study site basin area is 65,310 m^2, the highest peak located to the southeast is 628 m, with the lowest point of 529 m in the north-central portion of the enclosed basin (Figure 5), and a depth of 99 m (Table 1). The mean slope value for the South study site is 23.2°, the minimum slope value is 3.7°, and the maximum slope value is 38.9° (Table 2).

Table 2: Slope summaries in degrees for study sites and SML-173

Study Site	Min. Slope	Max. Slope	Mean Slope	Std. Dev.
North	1.8	34.5	18.5	8.5
East	0.5	46.9	19.5	8.9
Central	4.8	31.3	18.2	6.1
South	3.7	38.9	23.2	8.3
West	0.5	41.8	22.1	9.1
$\bar{x}$ of Study Sites	2.26	38.68	20.3	8.18
SML-173	0	57.3	19.6	9.8

Fig 6: West study site cockpit with corridor to the north (top), triangle is highest peak (east), red circle is lowest point, blue polygon is the basin, and contours are 5-meter interval. The base raster layer is a satellite image. Scale varies in this perspective view

The last sampled study site is located in the West and has a basin area of 134,249 m^2, the highest peak is 559 m, the lowest point is 438 m, with a depth of 121 m (Table 1). The minimum slope for the West study site is 0.5°, maximum slope 41.8°, mean of 22.1°, and a standard deviation of 9.1 (Table 2).

Discussion

SML-173 is characteristic of a true karst landscape because it is composed of massive soluble limestone, containing numerous caves and enclosed depressions, and the absence of surface water. The high standard deviation (100 m) in elevation reflects a large amount of variation in the DSM cells within SML-173. The substantial number of drainage basins (1,158) is indicative of tropical polygonal karst landscapes (Williams, 1972; Gunn, 1983; Day, 2004; Huang *et al*., 2014) [12, 13, 14, 15].

The 30-meter spatial resolution of the DSM limits the scale of landform analysis. For example, many cockpits and glades are drained by smaller sinkholes which will not resolve at the scale of the raster elevation model used in this study. The 512 sinks or topographically low spots occur in the floors of cockpits as described in the results but can also appear in glades. Sinks may also occur on corridors and saddles due to flow convergence associated with topographically higher cells on slopes adjacent to these landforms.

The East study site cockpit has a corridor entrance to from the west. The top of the corridor has a concave (yellow) structure, and that concavity extends down into the cockpit floor to the east and steep convex (red) slopes surround the cockpit floor (Figure 3). There are three saddles and one corridor associated with the East study site and it is these geomorphic features that give cockpit karst their distinctive appearance from an oblique view.

Slope values for the Central cockpit have the lowest standard deviation of 6.1 compared to the average of 8.18 for all sample study sites slopes (Figure 2). The Central cockpit has the highest minimum slope value 4.8° and is possibly due to the small area size of the cockpit floor and adjacent steep slopes illustrated in the cross-section profile (Figure 4, bottom).

There are two remarkable statistics for the South study site. First, the highest peak for the five sampled study sites occurs in the study site buffer zone and corresponds to the gradual increase in elevation from north to south across SML-173. Second, this site also contains the highest mean slope value of 23.2°. Additionally, there are seven high-elevation low-slope peaks creating numerous saddles (Figure 5) and a corridor entrance to the northwest making this a morphometrically complicated cockpit.

The West study site contains the deepest cockpit at 121 m which is 24.7% greater than the mean depth (Table 1) and has the largest standard deviation at 9.1 about 10% higher than the average (Table 2). There are eleven peaks connected to these slopes creating numerous saddles surrounding this cockpit.

There are approximately 150 of the 1,158 basin polygons affected by the SML-173 study area polygon in geoprocessing such as flow direction, flow accumulation, and clipping. Figure (Figure 2) illustrates small basins adjacent to the Arterial Road in the northeast section of SML-173 that were clipped by the study area polygon or affected by urban development.

Bauxite mining in SML-173 will negatively affect the hydrology and biodiversity of karst landforms in particular cockpits, glades, and corridors. These landforms will experience lowered elevations, steeper slopes, and decreased soil water storage capacity. Bauxite ore extraction begins with the removal of vegetation and the soil 'A' horizon. Ore removal is typically down to bedrock thus lowering elevation by several meters and as a result significantly steepening the lowland landscape making it more problematic to farm in the future. The hydrological and biological services provided by the karst landscape, to humans and nature, in SML-173 is under imminent threat of destruction from bauxite mining.

The debate over the boundary of the CCPA has been in the public domain for a number of years and that is an environmental issue for the citizens of Jamaica, the government, and the bauxite mining industry. The geomorphological evidence provided in this paper demonstrates that much of the land in SML-173, especially Trelawny and the southwest, are an extension of the Cockpit Country.

Conclusion

The five sampled study sites from SML-173 contain landforms associated with tropical cockpit karst landscape. Each of the sampled site includes corridors that connect cockpits and glades, saddles, and large enclosed depressions surrounded by limestone hills with multiple peaks. Figure 1 illustrates the overall nature of the landscape as a polygonal karst terrain using ridge lines. Figures 2 – 6 exemplify various geomorphic characteristics of each cockpit to provide visual evidence of karst landforms using basins, curvature, profile, 3d views, slope, and contours.

Depth and slope values within the study sites correspond with previously published literature for cockpit karst landscapes. Aub (1969) [3] stated cockpits range from 30 m to 150 m deep and this study found cockpit depths ranging from 87 m to 121 m. Sweeting (1958) [8] reported cockpit slopes ranging from 30° - 40° where this study found a mean slope of 20.3°, mean maximum slope of 38.7°, and a low standard deviation of 8.18. The actual steepness of the slopes, especially cliffs, is obscured by the dense tropical vegetation from which the DSM is derived. Furthermore, previous studies (Aub, 1969; Monroe, 1972; Versey, 1972) [3, 5, 7] have shown slopes surrounding cockpit floors are steep and convex as observed in this study (Figure 3).

Acknowledgements

This research was funded by Jacksonville State University (JSU) College of Science and Mathematics McCleur Scholars Program. I would like to thank Susan Koenig of the Windsor Research Centre in Trelawny Jamaica for assistance with SML-173 topics. I am grateful for the intellectual guidance on tropical karst landforms offered by Dr. Mick Day.

References

1. Miller D. Karst geomorphology of the white limestone group. Cainozoic research. 2003;3(1/2):189-219.
2. Sawkins JG, Wall GP, Barrett L, Lennox A, Hoffmann L, Brown CB, Etheridge R. Geological Survey of Great Britain. Reports on the geology of Jamaica, Part II of the West Indian Survey (Ser. Memoirs of the geological survey). Printed for H.M. Stationery Office., Longmans

Green, 1869, 1-339.
3. Aub C. The nature of cockpits and other depressions in the karst of Jamaica. Proceedings of the Fifth International Speleological Congress, Stuttgart 1969; Paper M15:1-7.
4. Smith DI, Drew DP, Atkinson TC. Hypotheses of karst landform development in Jamaica. Trans. Cave Research Group of Great Britain. 1972;14(2):159-173.
5. Monroe WH. A Glossary of Karst Terminology. USGS Water Supply Paper 1899-K, 1970, 26 pages.
6. Chenoweth MS. Developing a spatial database for the interpretation of Karst landscape and vegetation in the Jamaican Cockpit Country. Ph.D. Dissertation, University of Wisconsin – Milwaukee, 2003, 131 pages.
7. Versey HR. Karst in Jamaica. In: Herak M, Springfield VT, (editors). Important Karst Regions of the Northern Hemisphere. Elsevier, New York, 1972, 445-466.
8. Sweeting MM. The karstlands of Jamaica. The Geographical Journal. 1958;124(2):184-199.
9. Lyew-Ayee P, Viles HA, Tucker GE. The use of GIS-based digital morphometric techniques in the study of cockpit karst. Earth Surface Processes and Landforms. 2007;32(2):165-179.
10. Advanced Land Observing Satellite (ALOS, DAICHI) - PRISM Remote Sensing Instrument Stereo Mapping Description. Japan Aerospace Exploration Agency (JAXA). https://www.eorc.jaxa.jp/ALOS/en/index_e.htm. 18 June, 2022.
11. ArcGIS Online, 2021. https://services6.arcgis.com/3R3y1KXaPJ9BFnsU/arcgis/rest/services/Cockpit_sites/FeatureServer. 12 May, 2021.
12. Williams PW. Morphometric analysis of polygonal karst in New Guinea. Geological Society of America Bulletin. 1972;83(3):761-796.
13. Gunn J. Point-recharge of limestone aquifers - a model from New Zealand karst. Journal of Hydrology. 1983;61(1-3):19-29.
14. Day M. Morphometry of karst. In: Gunn J (editor) Encyclopedia of Caves and Karst Science. Fitzroy Dearborn, New York, 2004, 526-527.
15. Huang W, Deng C, Day MJ. Differentiating tower karst (fenglin) and cockpit karst (fengcong) using DEM contour, slope, and centroid. Environmental Earth Sciences. 2014;72(2):407-416.
16. Day M. The morphology and hydrology of some Jamaican karst depressions. Earth Surface Processes. 1976;1(2):111-129.
17. Day M. Limestone valley systems in north central Jamaica. Caribbean Geography. 1985;2(1):16-32.